Flavodiiron Proteins Promote Fast and Transient O 2 Photoreduction in Chlamydomonas

Frédéric Chaux, Adrien Burlacot, Malika Mekhalfi, Pascaline Auroy, Stéphanie Blangy, Pierre Richaud, G. Peltier

Flavodiiron Proteins Promote Fast and Transient O_2 Photoreduction in *Chlamydomonas*[1][OPEN]

Frédéric Chaux,[2] Adrien Burlacot,[2] Malika Mekhalfi, Pascaline Auroy, Stéphanie Blangy, Pierre Richaud, and Gilles Peltier[3]

CEA, CNRS, Aix-Marseille Université, Institut de Biosciences et Biotechnologies Aix-Marseille, UMR 7265, Laboratoire de Bioénergétique et Biotechnologie des Bactéries et Microalgues, CEA Cadarache, Saint-Paul-lez-Durance, F-13108 France

ORCID IDs: 0000-0001-7434-6416 (A.B.); 0000-0002-2226-3931 (G.P.).

During oxygenic photosynthesis, the reducing power generated by light energy conversion is mainly used to reduce carbon dioxide. In bacteria and archae, flavodiiron (Flv) proteins catalyze O_2 or NO reduction, thus protecting cells against oxidative or nitrosative stress. These proteins are found in cyanobacteria, mosses, and microalgae, but have been lost in angiosperms. Here, we used chlorophyll fluorescence and oxygen exchange measurement using [^{18}O]-labeled O_2 and a membrane inlet mass spectrometer to characterize *Chlamydomonas reinhardtii flvB* insertion mutants devoid of both FlvB and FlvA proteins. We show that Flv proteins are involved in a photo-dependent electron flow to oxygen, which drives most of the photosynthetic electron flow during the induction of photosynthesis. As a consequence, the chlorophyll fluorescence patterns are strongly affected in *flvB* mutants during a light transient, showing a lower PSII operating yield and a slower nonphotochemical quenching induction. Photoautotrophic growth of *flvB* mutants was indistinguishable from the wild type under constant light, but severely impaired under fluctuating light due to PSI photo damage. Remarkably, net photosynthesis of *flv* mutants was higher than in the wild type during the initial hour of a fluctuating light regime, but this advantage vanished under long-term exposure, and turned into PSI photo damage, thus explaining the marked growth retardation observed in these conditions. We conclude that the *C. reinhardtii* Flv participates in a Mehler-like reduction of O_2, which drives a large part of the photosynthetic electron flow during a light transient and is thus critical for growth under fluctuating light regimes.

Oxygenic photosynthesis, by reducing CO_2 into biomass and using water as an electron donor, is responsible for the major entry of carbon into ecosystems. During oxygenic photosynthesis, electrons originating from water splitting at PSII are transferred to PSI, which reduces $NADP^+$ into NADPH at its acceptor side. Electron transfer reactions generate as well a proton motive force (*pmf*) that drives the ATP synthesis. ATP and NADPH are then used to fuel the CO_2 photoreduction cycle. Although the main flow of electrons generated by oxygenic photosynthesis is used for CO_2 assimilation, it was early recognized that a significant part of electrons is diverted to molecular oxygen (Mehler, 1951; Radmer and Kok, 1976). Different mechanisms of light-dependent O_2 consumption have been described in the chloroplast, including direct O_2 photoreduction at the PSI acceptor side (also called Mehler reactions), the oxygenase activity of Rubisco (also called photorespiration), or the reduction of O_2 by the plastidial terminal oxidase PTOX (also called chlororespiration). The respective contribution of these different pathways has been a matter of debate and may considerably vary depending on the experimental conditions and according to the organisms considered (Badger et al., 2000). The physiological function of the different O_2 photoreduction pathways has been controversial, since they have been alternatively viewed as futile pathways resulting in a waste of energy, as protective mechanisms avoiding photooxidative damage, or as a mean to (re)-equilibrate the balance between reducing and phosphorylating powers through pseudocyclic photophosphorylations (Badger, 1985; Allen, 2003). In cyanobacteria, flavodiiron proteins catalyze NADPH-dependent reduction of O_2 at the PSI acceptor side (Vicente et al., 2002; Helman et al., 2003; Allahverdiyeva et al., 2013). The *Synechocystis* sp. PCC 6803 genome harbors four *Flv* genes, two of them (*Flv1* and *Flv3*) encoding proteins that form a functional heterodimer catalyzing O_2 photoreduction (Helman et al., 2003) and allowing growth under fluctuating light (Allahverdiyeva et al., 2011). The two others (*Flv2* and *Flv4*) code for proteins protecting PSII from over-reduction (Zhang et al., 2009, 2012) by using a

[1] This work was supported by the ERA-SynBio project Sun2Chem, and by the A*MIDEX (ANR-11-IDEX-0001-02) project. F.C. was recipient of a PhD grant of the CEA Tech Division of the "Commissariat à l'Energie Atomique et aux Energies Alternatives."

[2] These authors contributed equally to the article.

[3] Address correspondence to gilles.peltier@cea.fr.

The author responsible for distribution of materials integral to the findings presented in this article in accordance with the policy described in the Instructions for Authors (www.plantphysiol.org) is: Gilles Peltier (gilles.peltier@cea.fr).

F.C., A.B., and G.P. conceived the original research plans; F.C, A.B., M.M., P.A., and S.B. performed the experiments; F.C., A.B., P. R., and G.P. analyzed the data; F.C., A.B., and G.P. wrote the article.

[OPEN] Articles can be viewed without a subscription.

www.plantphysiol.org/cgi/doi/10.1104/pp.17.00421

yet-unidentified electron acceptor (Allahverdiyeva et al., 2015). *Flv* genes have been conserved in microalgae, mosses, and gymnosperms, but are notably absent from angiosperms genomes.

In Arabidopsis (*Arabidopsis thaliana*), the capacity to grow under fluctuating light depends on a strict regulation of the photosynthetic electron flow by the proton gradient, so-called photosynthetic control, which depends on the activity of cyclic electron flow (CEF) around PSI mediated by PGR5 and PGRL1 (Munekage et al., 2002; DalCorso et al., 2008; Suorsa et al., 2012). In cyanobacteria, the PGR5/PGRL1-dependent CEF is not functional, and it was proposed that growth under fluctuating light relies on the presence of Flv1 and Flv3 that would act as an electron sink preventing overreduction of PSI acceptors and production of reactive oxygen species (Allahverdiyeva et al., 2013). Algae and mosses harbor both Flvs and PGRL1/PGR5 CEF components (Tolleter et al., 2011; Dang et al., 2014; Johnson et al., 2014; Gerotto et al., 2016). Based on the accumulation of Flv proteins in a *Chlamydomonas reinhardtii* mutant (*pgrl1*) lacking photosynthetic control due to a deficiency in CEF, it was suggested that Flvs are induced to catalyze O_2 photoreduction when PSI acceptors are overreduced (Dang et al., 2014). More recently, Flv mutants have been characterized in the moss *Physcomitrella patens* (Gerotto et al., 2016) and in the liverwort *Marchantia* (Shimakawa et al., 2017), showing that these proteins are involved in alternative electron flow and are required for growth of the moss under fluctuating light. However, so far there is no experimental evidence for a Flv-mediated oxygen photoreduction in eukaryotic microalgae (Curien et al., 2016).

With the aim to better understand the function of Flvs in microalgal photosynthesis, and particularly to determine whether oxygen is the electron acceptor of Flv and what part of the electron flow is diverted toward oxygen photoreduction during photosynthesis, we study here *C. reinhardtii flvB* insertion mutants of the *Chlamydomonas* Library Project (CLiP) library (Li et al., 2016) devoid of both FlvB and FlvA proteins. By performing photosynthetic gas exchange measurements using [^{18}O]-labeled O_2 and a membrane inlet mass spectrometer (MIMS), we show that O_2 photoreduction is strongly decreased in *flv* mutants, particularly during the induction phase of photosynthesis. We conclude that FlvA and FlvB proteins are involved in a Mehler-like O_2 photoreduction, which massively drives electrons to O_2 during the induction phase of photosynthesis.

RESULTS

Identification and Preliminary Characterization of Four Independent *C. reinhardtii flvB* Mutants

To investigate the function of Flvs in the unicellular alga *C. reinhardtii*, we searched for insertion mutants in the *Flvb* (Cre16.g691800) gene region in the CLiP library (https://www.chlamylibrary.org; Li et al., 2016). We obtained four putative *flvB* mutants, three holding insertion of the paromomycin resistance cassette in introns and one with a possible large deletion (Fig. 1A; Supplemental Table S1). All strains grew normally on Tris-acetate-phosphate or minimal medium under constant low light (40 μmol photons m^{-2} s^{-1}). Insertion was confirmed by performing PCR on genomic DNA of *flvB-14*, *flvB-208*, and *flvB-308* (Supplemental Fig. S1). We did not, however, succeed in mapping the insertion in the putative *flvB-21* mutant, possibly due to atypical genomic rearrangement(s) that may occur with cassette insertion (Li et al., 2016). Immunodetection was then performed on total whole-cell protein extracts by using antibodies directed against recombinant FlvB and FlvA proteins (Fig. 1, B and C). FlvB and FlvA were not detected in the three independent *flvB-21*, *flvB-208*, and *flvB-308* strains, while a low level was detected in *flvB-14* (hereafter called knockdown mutant). The difference in protein accumulation observed in *flvB-208* and *flvB-14* is surprising, since insertions are located in the same intron (Fig. 1A). This might be due to a differential effect on intron splicing depending on the location of the insertion in the intron. Similar patterns of accumulation were previously observed for the Flv1 protein in the *Synechocystis flv3* mutant (Allahverdiyeva et al., 2013) and for the FlvA protein in the *P. patens flvb* mutant (Gerotto et al., 2016), which were interpreted by the existence of a functional heterodimer between Flv1 and Flv3 in *Synechocystis* and between FlvA and FlvB in *P. patens*.

Chlorophyll Fluorescence Transients Are Strongly Affected under High Light in *flvB* Mutants

To determine how electron transfer reactions are affected in *flvB* mutants, we recorded chlorophyll fluorescence transients under different light intensities. Under low actinic light (25 μmol photons m^{-2} s^{-1}), no difference could be recorded between *flvB* mutants and the CC-4533 strain, hereafter referred to as the wild type (Fig. 2A). However, upon exposure to higher light intensities (100 or 500 μmol photons m^{-2} s^{-1}), a marked difference was observed between *flvB* mutants and the control wild-type strain, the fluorescence signal transiently reaching a much higher value in the mutants than in the wild type (Fig. 2, B and C). The PSII operating yield measured after 20 s of actinic illumination was much lower in *flvB* mutants than in the wild type, but the difference partially vanished after 5 min of light exposure (Fig. 3). A smaller effect was observed in *flvB-14*, which accumulates low levels of FlvB and FlvA (Fig. 2B; Supplemental Fig. S2). Interestingly, relaxation of chlorophyll fluorescence to a steady-state level after a saturating flash was slower in the *flvB* mutants than in the wild-type strain (Supplemental Fig. S3), indicating that Flv proteins are functional during brief light transients. We conclude from these chlorophyll fluorescence measurements that Flv proteins are involved in photosynthetic electron transfer reactions, particularly

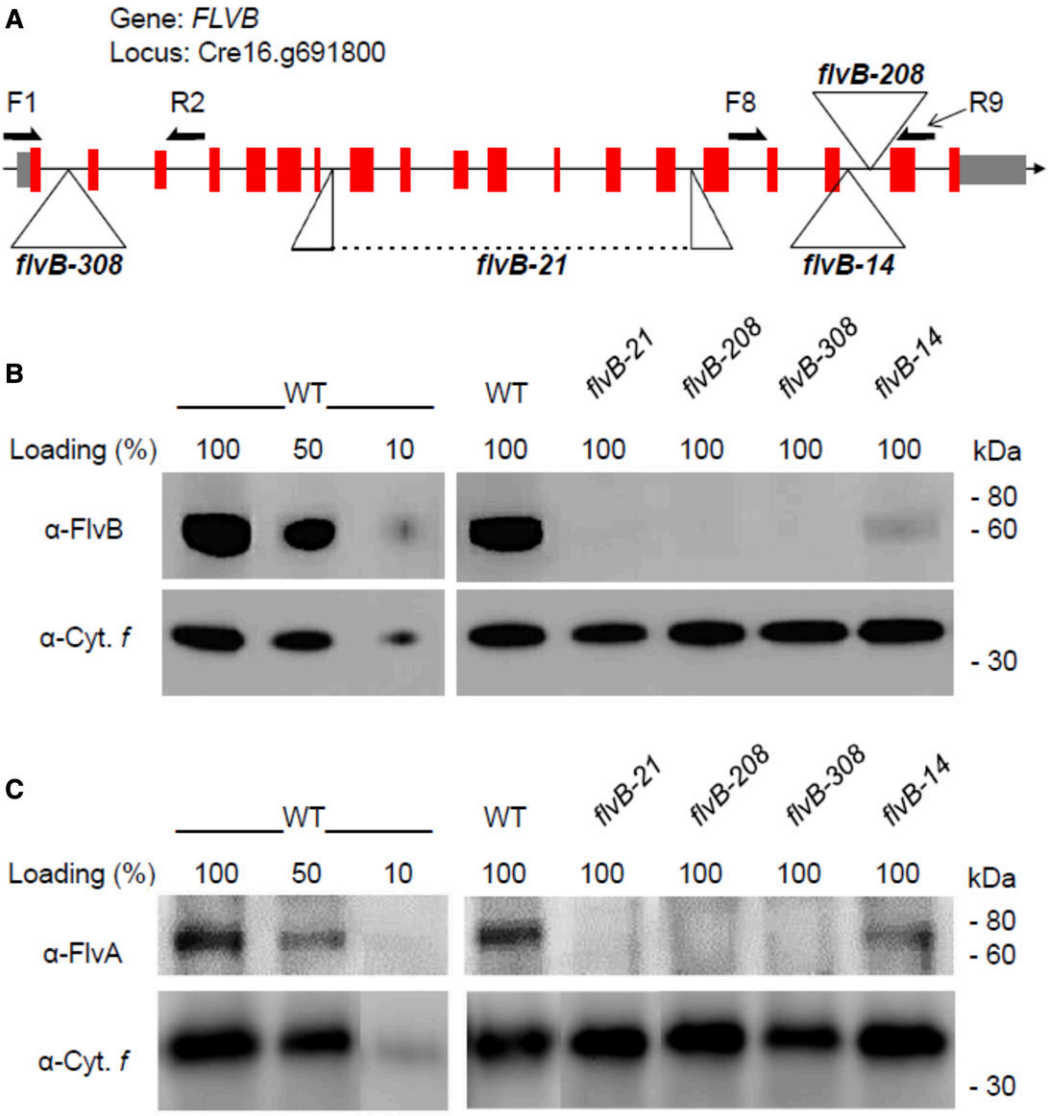

Figure 1. Characterization of independent *C. reinhardtii* mutants carrying an insertion in the *flvB* gene. A, Four mutant strains from the CLiP (www.chlamylibrary.org/) harboring putative insertions of the paromomycin resistance cassette in the *FLVB* locus (Cre16.g691800) were characterized. Exons, introns, and untranslated regions are shown as red boxes, black lines, and gray boxes, respectively. Genomic sequences flanking the insertion cassette of the four putative *flvB* mutant strains obtained from the CLiP Web site were used to design primers (F1/R2 and F8/R9) to confirm the location of insertion. B and C, Immunoanalysis of FlvB and FlvA protein amounts were carried out using antibodies produced against recombinant FlvB (B) and FlvA (C) proteins, respectively. A cytochrome *f* antibody was used as loading control.

during the induction phase of photosynthesis under moderate or high illumination.

Flv Proteins Interact with the Photosynthetic Electron Transport Chain at the Level of PSI Acceptors

To better characterize the site of interaction between Flv proteins and the photosynthetic electron transport chain, we first used DBMIB, a photosynthetic electron flow inhibitor acting at the Q_0 site of the cytochrome b_6f complex. Upon addition of DBMIB, the chlorophyll fluorescence level rapidly rose to the maximal fluorescence level (F_M) with similar light induction curves in the wild type and *flvB* mutants (Fig. 4), thus indicating that Flv proteins interact with the photosynthetic electron transport chain downstream the cytochrome b_6f. We then used oxidized methyl viologen (MV), which efficiently accepts electrons at the PSI acceptor side. The chlorophyll fluorescence induction curve of the wild type was only slightly affected by MV (Fig. 4). In contrast, the strong chlorophyll fluorescence increase observed in the *flvB* mutant was suppressed by the MV treatment, thus indicating that the site of action of Flv is located downstream the action site of MV, which is at the PSI acceptor

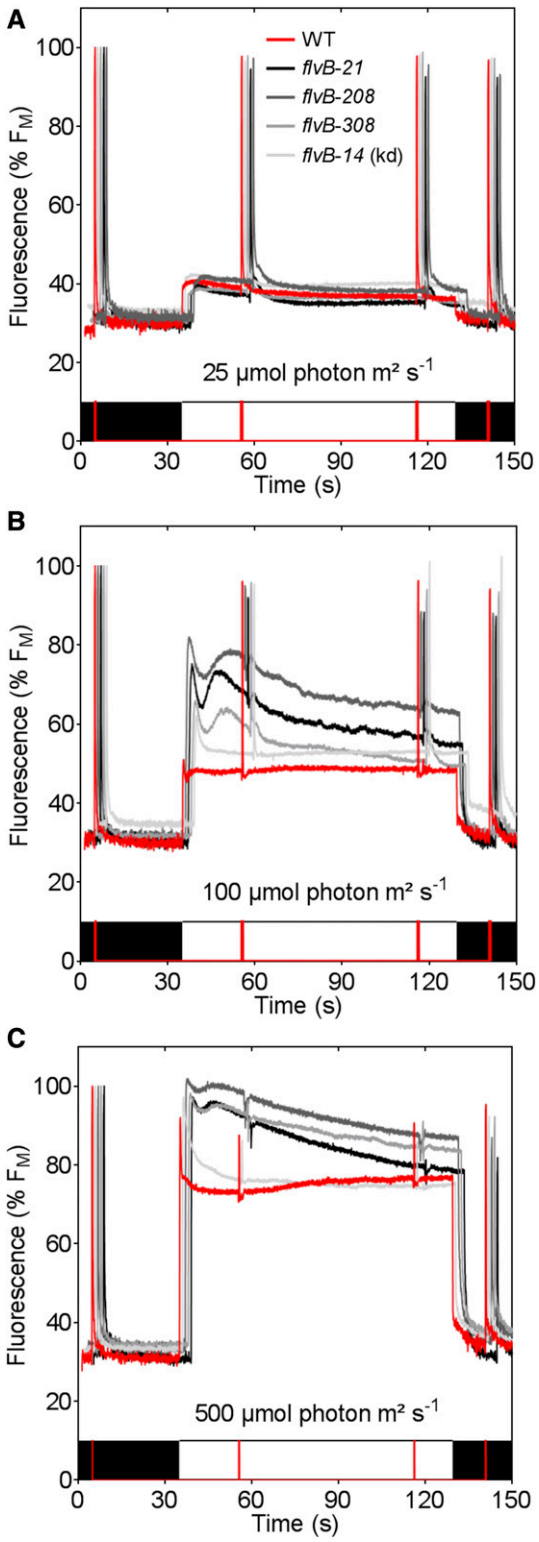

Figure 2. Chlorophyll fluorescence measurements during dark to light transients in *C. reinhardtii* wild type (WT) and *flvB* mutant strains. Cells were grown in HSM medium under low light (40 μmol photon m^{-2} s^{-1}) and harvested during exponential phase. Chlorophyll fluorescence measurements were performed using pulse amplitude modulated fluorimeter in the dark (black boxes) and under red actinic light (white boxes) of different intensities: 25 μmol photon m^{-2} s^{-1} (A), 100 μmol photon m^{-2} s^{-1} (B), and 500 μmol photon m^{-2} s^{-1} (C). Saturating flashes were supplied when indicated by red vertical lines. Data are normalized on initial F_M measurements and traces of mutant strains are shifted few seconds to the right for clarity.

side level. Altogether, these observations also show that Flv proteins are active in highly reducing conditions and that its activity is decreased when the reducing pressure is low.

Oxygen Photoreduction Is Strongly Reduced in *flvB* Mutants

We then measured O_2 exchange during light transients using a MIMS and [^{18}O]-labeled O_2 (Fig. 5). This technique allows discriminating unidirectional fluxes of O_2 in the light: *i*, gross O_2 evolution, which represents O_2 produced by PSII, and *ii*, O_2 uptake in the light, which consists in different mechanisms such as O_2 photoreduction and mitochondrial respiration. In such experiments, O_2-consuming processes take up all O_2 species present in the medium including [^{18}O]-labeled O_2, while photosynthesis will essentially produce non-labeled O_2 from water-splitting at PSII. When light was switched on, the O_2 uptake rate strongly increased in the wild type, and then progressively declined during the light period (Fig. 5A). In the *flvB-21* mutant, the O_2 uptake rate measured in the light was much lower than in the wild type and remained constant throughout the light period (Fig. 5B), thus showing that Flv proteins are involved in O_2 photoreduction. The O_2 uptake rate remained constant throughout the light period in *flvB* mutants and was close to the O_2 exchange rate measured in the dark, which is mainly due in *Chlamydomonas* to persistent mitochondrial respiration (Peltier and Thibault, 1985b). Therefore, the large O_2 uptake component observed in the wild type during the first minutes of illumination is mainly due to the activity of Flv proteins. Gross O_2 evolution was also reduced in the *flvB-21* mutant as compared to the wild type, indicating that in the wild type Flv-mediated O_2 photoreduction promotes an extra-electron flow from PSII to O_2. Similar effects were observed in the three independent *flvB* mutants (*flvB-21*, *flvB-208*, and *flvB-308*), while an intermediary effect was observed in the *flvB-14* knockdown strain (Fig. 5, C and D). Dark O_2 uptake rates measured in the different strains before and after the illumination period did not show significant differences (Supplemental Fig. S4). The net O_2 evolution rate measured after 5 min of illumination, which reflects net photosynthesis due to CO_2 reduction, was not much affected in the mutant as compared to the wild type (Fig. 5D). This shows that Flv-dependent O_2 photoreduction does not efficiently compete with CO_2 fixation during steady-state photosynthesis. Note that after 5 min of illumination, O_2

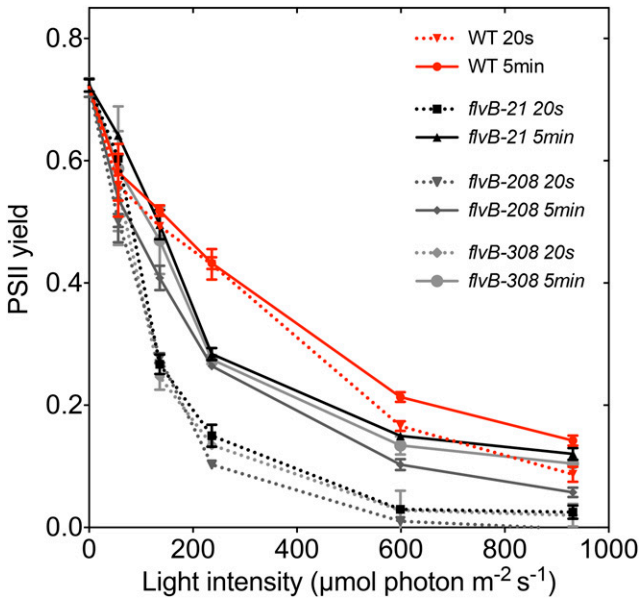

Figure 3. Light dependence of the PSII yield in the wild type (WT) and *flvB* mutant strains. Upon 10-min dark adaptation under constant air bubbling, algal suspensions of wild type and *flvB* mutant strains were introduced in the cuvette of a pulse amplitude-modulated fluorimeter. PSII yields were measured after 20 s (dotted lines) or 5 min (plain lines) of illumination at different light intensities. Shown are the mean values (±SD, $n = 3$).

uptake rates remained slightly higher in the wild type as compared to *flvB* mutant strains (Fig. 5D), indicating that the Flv-mediated electron flow to O_2 also contributes under steady-state illumination. We conclude from these experiments that O_2 photoreduction primes and replaces CO_2 fixation during the induction phase of photosynthesis in *C. reinhardtii*, as was previously reported in *Scenedesmus obliquus* and *Anacystis nidulans* (Radmer and Kok, 1976), and we further establish that Flv proteins are involved in this phenomenon.

Growth of *flvB* Mutants Is Delayed under Fluctuating Light Conditions Due to PSI Impairment

The strong effect observed in *flvB* mutants during the induction phase of photosynthesis and the growth delay previously reported in Δ*flv* cyanobacterial mutants grown under fluctuating light (Allahverdiyeva et al., 2011) prompted us to analyze growth performances under repeated light changes. When *C. reinhardtii* cells were grown under 5 min low light (50 µmol photons m^{-2} s^{-1}) and 1 min high light (500 µmol photons m^{-2} s^{-1}), a strong growth retardation was observed in the three *flvB* mutant strains (*flvB-21*, *flvB-208*, and *flvB-308*) as compared to the wild type, while an intermediary effect was observed in the *flvB-14* strain (Fig. 6A). This drastic effect on growth did not, however, lead to cell death, since growth recovery was observed during a subsequent growth period under continuous light (Supplemental Fig. S5). In contrast, no growth difference could be observed between mutant and wild-type strains under constant illumination, even under high light intensity (800 µmol photons m^{-2} s^{-1}; Fig. 6A). To understand the mechanism underlying growth retardation, we performed PSII and PSI activity measurements at different time points during exposure to fluctuating light conditions (Fig. 6B). Maximal PSII activity was slightly decreased (by about 20%) in the *flvB* mutant upon 48 h of fluctuating light exposure, but a drastic decrease of the PSI activity (about 80%) was observed in the mutant (Fig. 6B). Immunoanalysis of PSII and PSI subunits, respectively PsbA and PsaD, revealed no major change in the PsbA subunit amount, but a large decrease in PsaD in the *flvB* mutant upon 24 h of exposure to fluctuating light (Fig. 6C). We conclude from this experiment that repeated transitions from low to high light induce PSI photoinhibition in the absence of Flv-mediated electron flow.

Defect in Flv Has Ambivalent Effects on Photosynthesis

To better characterize the function of Flv proteins during photosynthesis, we measured photosynthetic O_2 exchange in cells during exposure to a fluctuating light regime (Fig. 7). Net photosynthesis was higher in *flvB*

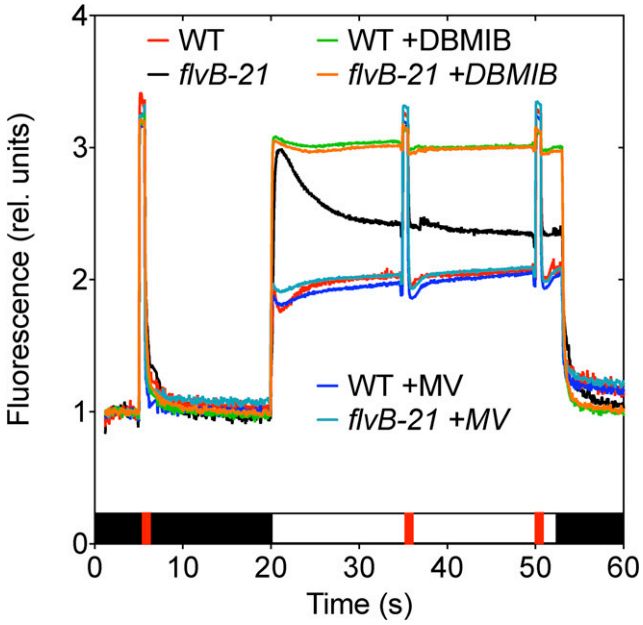

Figure 4. Effect of DBMIB and MV on chlorophyll fluorescence transients measured in wild type (WT) and *flvB* mutant strains. Samples were placed in the dark (black box) in the presence of 1 µM DBMIB, 1 mM MV, or without addition of any chemicals. Chlorophyll fluorescence was measured during a transient dark to light (100 µmol photon m^{-2} s^{-1}) transient. Saturating flashes were supplied when indicated by red vertical lines. Shown are the traces representative of $n = 2$ independent measurements. Fluorescence data have been normalized on F_0.

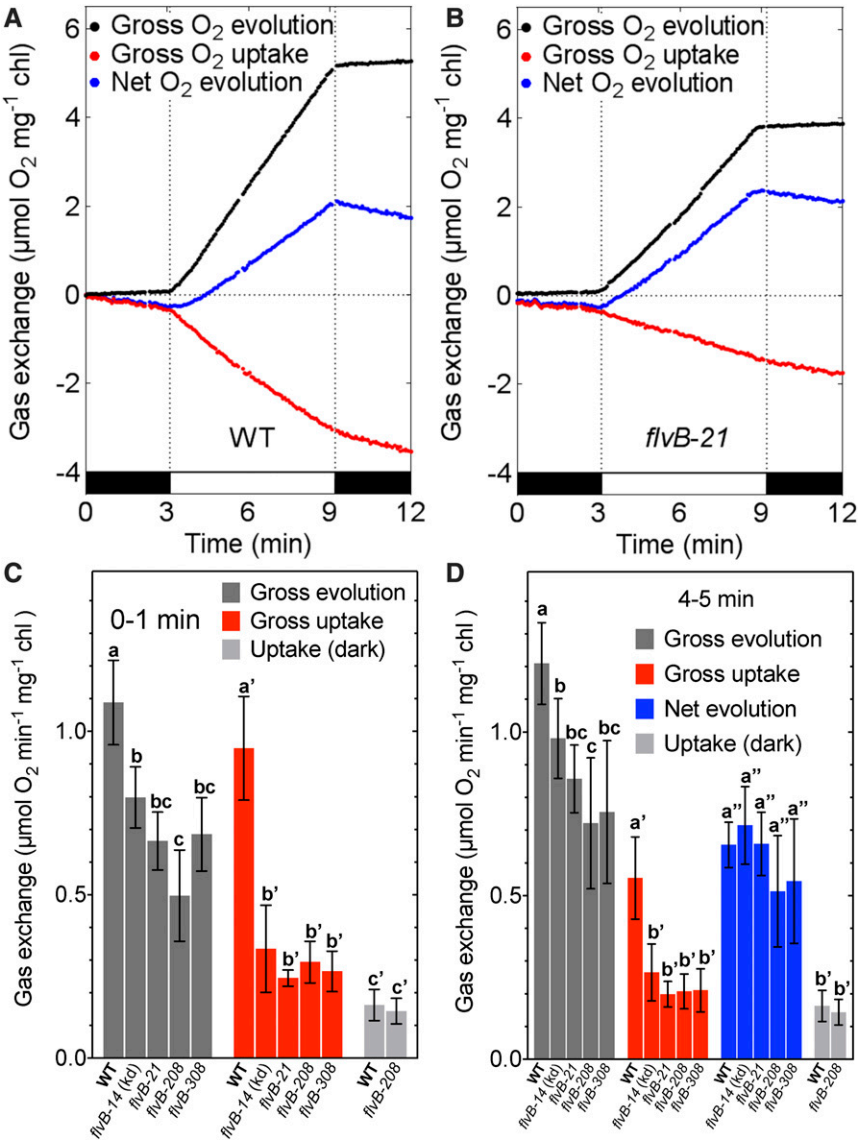

Figure 5. Oxygen exchange measurements performed using a MIMS and ^{18}O-labeled O_2 in the wild type (WT) and *flvB* mutant strains. A and B, Gross O_2 evolution (black dots), O_2 uptake (red dots), and net O_2 production (blue dots) were determined in the wild type (A) and the *flvB-21* mutant (B). C, Mean values of gross O_2 evolution (dark gray boxes) and O_2 uptake (red boxes) measured during the first minute of illumination (shown are means ± SD, $n = 3$) in the wild type, and in *flvB-14*, *flvB-21*, *flvB-208*, and *flvB-308* mutant strains. D, Mean values of gross O_2 evolution (dark gray boxes), O_2 uptake (red boxes), and net O_2 evolution (blue boxes) measured between 4 and 5 min of illumination (shown are means ± SD, $n = 3$). Values of O_2 uptake in the dark prior to illumination (light gray boxes) are shown for the wild type and *flvB-208* (shown are means ± SD, $n = 3$) (C and D). Letters above the bars (C and D) represent statistically significant differences (P value < 0.05) between strains for a given gas exchange measurement based on ANOVA analysis (Tukey adjusted P value); letters with single or double quote have been used to group oxygen uptake or net evolution data respectively.

mutant cells during the first 30 min of a fluctuating light exposure as compared to the wild type (Fig. 7A), but the difference vanished after 1 h, and a negative effect was observed upon 4 h of fluctuating light exposure (Fig. 7C), in accordance with the inhibition of PSI (Fig. 6). In contrast, the O_2 uptake rate measured in the light was initially much lower in the *flvB* mutant than in the wild type (Figs. 5, A and B, and 7, B and D), but progressively increased in the mutant until reaching a similar level as in the wild type (Fig. 7D). This indicates that during the time-course of an exposure to a fluctuating light regime, a Flv-independent O_2 uptake process was progressively triggered in the mutant. Therefore, depending on the duration of a fluctuating light exposure, the loss of Flv proteins leads either to a positive or a negative effect on net photosynthesis, the positive effect being accompanied by a decrease in the O_2 uptake (mediated by Flv) and the negative effect being accompanied by a progressive increase in an O_2 uptake component. The induction of this Flv-independent, light-dependent O_2 uptake phenomenon likely results in ROS production, thus explaining growth retardation and PSI photoinhibition observed under long-term exposure (Fig. 6).

Nonphotochemical Quenching Induction Is Affected in *flvB* Mutant Strains

To better understand the impact of the Flv-mediated electron flow to O_2 on photosynthesis, we measured the nonphotochemical quenching (NPQ) induction in high light-adapted cells (Fig. 8A). During a dark to light transient, NPQ rapidly rose in the wild type to reach a steady-state level. NPQ induction was slower in the *flvB* mutant, but reached a similar level after 1 to 2 min of illumination (Fig. 8A). In *C. reinhardtii*, NPQ relies on

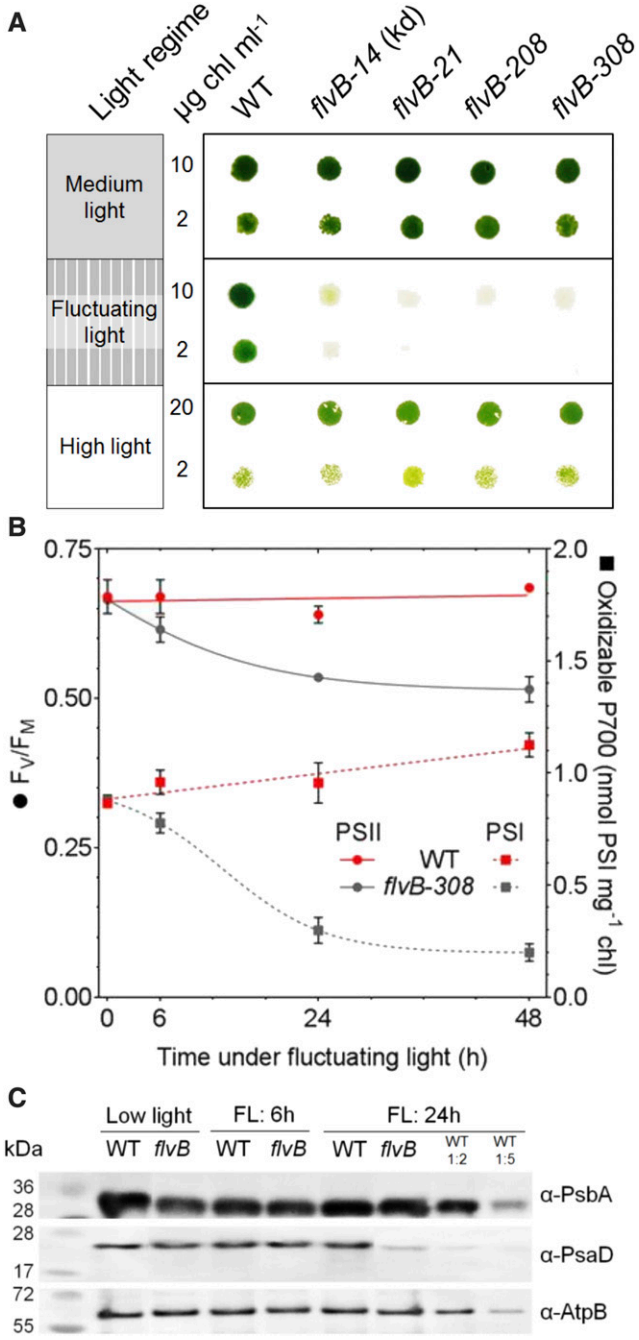

Figure 6. Growth and PSI activity of *flvB* mutants are impaired under fluctuating light. A, Cells were spotted on HSM agar plates and exposed for 10 d to continuous medium (125 μmol photon m^{-2} s^{-1}), high (800 μmol photon m^{-2} s^{-1}), or to fluctuating light intensity (alternatively 5 min at 50 μmol photon m^{-2} s^{-1} and 1 min at 500 μmol photon m^{-2} s^{-1}). Shown are representative drops of three independent spot tests. B, PSII and PSI activity measured in response to fluctuating light exposure. Wild-type (WT) and *flvB-308* cells were grown photoautotrophically in flasks under low light (50 μmol photon m^{-2} s^{-1}) and exposed at t_0 to fluctuating light cycles (5 min at 50 μmol photon m^{-2} s^{-1} and 1 min at 500 μmol photon m^{-2} s^{-1}) for 48 h. Maximal PSII yields and maximal oxidizable PSI were respectively determined by means of chlorophyll fluorescence and P700 absorption changes measurements PSII. C, Immunoanalysis of PSII and PSI subunit amounts in the wild type and *flvB-308* mutant in response to fluctuating light exposure. PsbA and PsaD antibodies were used to probe amounts of PSII and PSI complexes, respectively. AtpB antibody was used as loading control.

two factors: accumulation of the LHCSR3 protein and lumen acidification (Peers et al., 2009; Bonente et al., 2011). Since both wild-type and *flvB* mutant strains accumulated similar levels of the LHCSR3 protein (Fig. 8B), the slower induction of NPQ is likely due to a slower acidification of the lumen in *flvB* mutants as compared to the wild type. To further investigate effects on the proton gradient, we measured electrochromic carotenoid shift (ECS). In the *flvB* mutant, the *pmf* was decreased by one third and the ΔpH component by ~50% as compared to the wild type (Fig. 8C), the ratio between $\Delta\Psi$ and ΔpH components being unaffected (Supplemental Fig. S6). Moreover, time constant of ECS decay indicates that membrane conductivity to protons (g_H^+) is not altered in the *flvB* mutant, whereas proton flux ($\nu_H^+ = pmf * g_H^+$) is lower (Fig. 8D), suggesting a lower rate of ATP synthesis in the mutant during the induction of photosynthesis. We conclude from this experiment that the photosynthetic electron flow to O_2 mediated by Flv proteins participates in the wild type to the establishment of *pmf* that allows fast induction of the NPQ and higher ATP production during a light transient (Fig. 9A).

DISCUSSION

Flv Proteins Are Involved in O_2 Photoreduction during a Light Transient

By characterizing four independent insertion mutants of *C. reinhardtii* in the *Flvb* gene region affected in the accumulation of FlvB and FlvA proteins, we show here that Flv are involved in O_2 photoreduction at the acceptor side of PSI. Forty years ago, Radmer and Kok used [^{18}O]-labeled O_2 and mass spectrometry to show that in *Scenedesmus* and *Anacystis*, O_2 photoreduction primes and replaces CO_2 fixation during the induction of photosynthesis (Radmer and Kok, 1976), but mechanisms of O_2 photoreduction have remained elusive for a long time. Later studies showed that different mechanisms contribute to O_2 uptake in the light. Under steady-state conditions, persistent mitochondrial respiration in the light (Peltier and Thibault, 1985b) and a small contribution of photorespiration could be detected in *C. reinhardtii* (Peltier and Thibault, 1985a), the latter operating in microalgae at a much lower rate than in C_3 plants (Badger et al., 2000). We have shown here that Flv-mediated O_2 photoreduction drives most of the photosynthetic electron flow during the induction phase of photosynthesis in wild-type strains, when CO_2 assimilation has not started yet. Flv activity appears to be restricted to highly reducing conditions, which might result from a lower affinity to NADPH than the Calvin cycle enzymes, as recently proposed (Shikanai and Yamamoto, 2017).

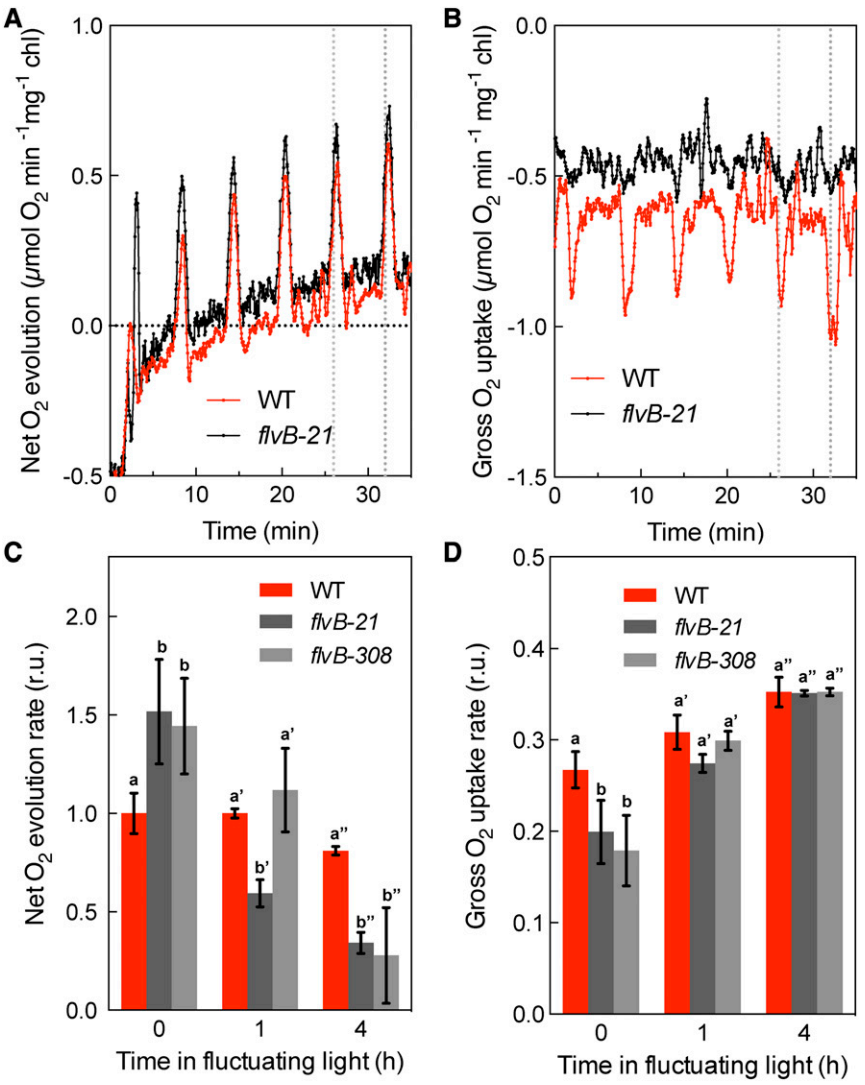

Figure 7. Net O_2 exchange measurements under fluctuating light in *flvB* mutants and in wild-type (WT) *C. reinhardtii* strains. Cells were grown photoautotrophically in air under continuous light (50 μmol photon m^{-2} s^{-1}) and then exposed up to 4 h to a fluctuating light regime (1 min at 50 μmol photon m^{-2} s^{-1}, 5 min at 500 μmol photon m^{-2} s^{-1}) before performing O_2 exchange measurements using a MIMS under similar fluctuating light conditions. A and B, Representative traces of net O_2 evolution rate (A) and O_2 uptake rate in the light (B) measured in the *flvB-21* mutant and wild type under fluctuating light in cells previously cultivated under continuous light. C and D, Mean values of net O_2 evolution (C) and O_2 uptake rates in the light (D) measured in fluctuating light in *flvB-21*, *flvB-308*, and wild-type strains. Shown are means (±SD, $n = 3$ for t = 0 h, $n = 2$ for t > 0 h) of net O_2 evolution rates relative to the wild type (at t = 0) and measured during the 5th light fluctuation period (as indicated in A and B by vertical dotted lines) in the wild type (red boxes) and *flvB* mutants (gray boxes). Letters (a and b) above the bars (C and D) represent statistically significant differences (P value < 0.05) between strains for a given gas exchange measurement based on ANOVA analysis; letters with simple or double quote have been used to group oxygen exchange data after 1 and 4 h or fluctuating light, respectively.

Chlamydomonas FlvA/FlvB Proteins Function in a Similar Manner as Cyanobacterial Flv1/Flv3

Phylogenetic analysis of the Flv family has shown that algal and mosses FlvB proteins are homologous to cyanobacterial Flv3 and Flv4, while FlvA proteins are homologous to cyanobacterial Flv1 and Flv2 (Zhang et al., 2009; Peltier et al., 2010). In *Synechocystis* PCC6803, Flv1 and Flv3 have been proposed to catalyze O_2 photoreduction into water without generation of ROS, and protect PSI from inhibition under fluctuating light (Allahverdiyeva et al., 2013). Based on O_2 photoreduction measurements in Δ*flv1* and Δ*flv3* cyanobacterial mutants, it was concluded that Flv3 function as a hetero-dimer with Flv1 (Helman et al., 2003; Allahverdiyeva et al., 2011). However, a functional Flv3 homo-oligomer may also be formed, as deduced from the overproduction of Flv3 in *Synechocystis* (Mustila et al., 2016). On the other hand, Flv2 and Flv4 protect PSII by a different mechanism and using a yet-uncharacterized electron acceptor (Zhang et al., 2012; Bersanini et al., 2014). From our data, we conclude that *C. reinhardtii* FlvA and FlvB are involved in O_2 photoreduction at the PSI acceptor side and therefore likely functions in a similar manner as cyanobacterial Flv1 and Flv3. Because the presence of Flv proteins prevents PSI photodamage, it is most likely that O_2 is fully reduced into water without production of ROS, as previously proposed for cyanobacteria (Helman et al., 2003). Based on the fact that FlvA could not be detected in *flvB* knockout mutants (Fig. 1C), we conclude that *C. reinhardtii* FlvA and FlvB proteins form in vivo a functional heterodimer, as previously proposed for Flv1 and Flv3 in *Synechocystis* (Helman et al., 2003; Allahverdiyeva et al., 2013) and FlvA and FlvB in *P. patens* (Gerotto et al., 2016).

Flv Proteins Are Involved in a Pseudocyclic Electron Flow to O_2 and Participates in the Establishment of a *pmf*

By mediating an electron flow from water to O_2 Flv proteins are involved in a pseudocyclic electron flow

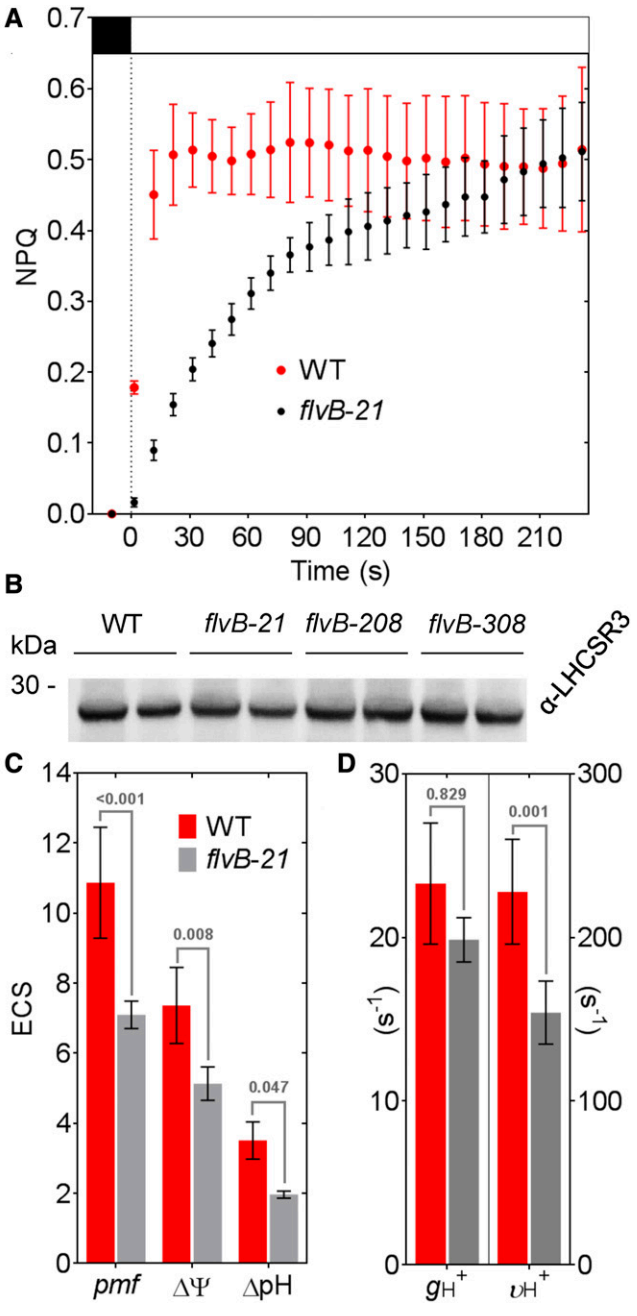

Figure 8. NPQ induction and proton motive force (*pmf*) measurements in the wild type (WT) and *flvB-21* mutant. A, For NPQ measurements, cells were exposed to 200 μmol photon m^{-2} s^{-1} for 4 h to induce accumulation of the LHCSR3 prior to chlorophyll fluorescence measurements. The wild type and *flvB-21* mutant were then exposed to 500 μmol photon m^{-2} s^{-1} in the PAM cuvette (white box) and NPQ determined from chlorophyll fluorescence measurements. NPQ values are the mean (±SD, $n = 3$) in the wild type (red symbols) and *flvB-21* mutant (black symbols). B, Immunodetection of LHCSR3 protein in experimental conditions as described in (A) in wild type and different *flvB* mutants. C, Different components of the *pmf* ($\Delta\Psi$ and ΔpH) were determined from ECS measurements in wild type (red) and *flvB-21* mutant (gray) from similar experiments as described in (Supplemental Fig. S5A). D, Membrane proton conductivity (g_H^+) and proton flow (ν_H^+) were determined from ECS measurements. Numbers above bars (C and D) represent uncorrected *P* values as determined by ANOVA using Fischer's LSD.

and therefore participates in the generation of a *pmf* (Fig. 8, C and D). In addition to its role in ATP synthesis, the *pmf* triggers two main mechanisms, the qE-type NPQ (LHCSR3-dependent) and the photosynthetic control, which participate in the regulation of the photosynthetic electron flow and protect PSI from acceptor-side limitations and PSI photoinhibition (Chaux et al., 2015, 2017). The CEF also participates in the establishment of a *pmf*, and its role in triggering both NPQ and the photosynthetic control has been established (Munekage et al., 2002; Joliot and Johnson, 2011; Tolleter et al., 2011; Suorsa et al., 2012). As shown here by the delayed induction of NPQ (Fig. 7A) measured in *flvB* mutants during a light transient, the Flv-mediated pseudocyclic electron flow to O_2 is involved in the rapid establishment of NPQ (Fig. 8A).

In *Chlamydomonas*, Flv-Mediated Electron Flow to O_2 Has Ambivalent Effects on Photosynthesis

Although no effect of Flv deficiency was observed on photosynthesis and growth under continuous illumination, ambivalent effects were observed upon exposure to fluctuating light. During a short-term exposure (<1 h) of fluctuating light, net photosynthesis was enhanced in *flvB* mutants as compared to the wild type. However, this advantage vanished thereafter, net photosynthesis being strongly decreased in the mutant (Fig. 7C). To understand such an ambivalent effect, we need to consider the different factors involved in the limitation of photosynthesis. Photosynthetic CO_2 fixation requires both NADPH and ATP, and a fine tune in the supply of both energy sources is needed for an optimal functioning of photosynthesis (Kramer and Evans, 2011). In other words, photosynthetic CO_2 fixation can be either limited by the NADPH supply or by the ATP supply. The Flv-mediated electron flow from PSII to O_2 has two effects on photosynthesis, one is to divert electrons toward O_2, therefore limiting the NADPH supply and the other to generate *pmf*, which may either be used to produce ATP and down-regulate the photosynthetic electron flow. Lack of Flv would therefore favor NADPH supply by two means: by avoiding the loss of electrons toward O_2 and by lowering the down-regulation of photosynthetic electron flow. A positive effect of a Flv defect on photosynthesis would therefore indicate that photosynthesis is limited by the supply of reducing power (high ATP/NADPH ratio), when cells switch from a continuous to a fluctuating light regime. However, in conditions where ATP is lacking (low ATP/NADPH ratio), the defect in Flv would enhance the disequilibrium by lowering ATP and increasing NADPH.

The ambivalent effect of Flv may therefore reveal the existence of different limitation regimes of photosynthesis (NADPH-limited versus ATP-limited) under fluctuating light conditions, a progressive switch from a NADPH-limited regime toward an ATP-limited regime occurring upon long-term exposure to fluctuating light.

In the absence of Flv, cells would produce more NADPH than strictly needed to make photosynthesis working at is optimal regime and would progressively accumulate an excess of reducing power. The 1-h retardation in the appearance of the negative effect would be due to the buffering capacity of intracellular metabolic pools and electron sinks. When the excess of NADPH produced exceeds the buffering capacity, overaccumulation of reducing power would result in the production of ROS and in turn to PSI photoinhibition (Fig. 6, B and C). A similar scenario based on a progressive disequilibrium between NADPH and ATP production was recently proposed to explain the delay between PSI photoinhibition and CO_2 when a double *C. reinhardtii* mutant deficient in CEF and qE was exposed to a sudden light increase (Chaux et al., 2017).

Compensation between Flvs-Mediated O_2 Photoreduction and PGRL1/PGR5-Dependent CEF

In the absence of CEF, *Arabidopsis pgr5* and *pgrl1* mutants are prone to PSI photoinhibition and severe growth retardation under high light (DalCorso et al., 2008; Munekage et al., 2008). The wild-type phenotype was restored in the *Arabidopsis pgr5* mutant by the expression of *P. patens* FlvA and FlvB proteins, thus showing that artificially rewiring the photosynthetic electron flow to O_2 through Flvs can compensate deficiency in CEF (Yamamoto et al., 2016). In *Synechocystis*, which lacks PGR5-PGRL1 CEF, deletion of Flv1 and Flv3 results in a severe decrease (about 60%) in net photosynthesis under constant high light (Allahverdiyeva et al., 2013). This strongly contrasts with *C. reinhardtii*, where no decrease in net photosynthesis was observed under constant light in *flvB* mutants (Fig. 5D). This difference may result from a compensation by the PGRL1/PGR5-dependent CEF, which like pseudocyclic electron flow generates extra-*pmf* and extra-ATP during photosynthesis. Indeed, deficiency in CEF in *C. reinhardtii* was partially compensated by an increase in Flv-dependent O_2 photoreduction (Dang et al., 2014). Therefore, Flv-dependent O_2 photoreduction and CEF appear as partially redundant mechanisms in microalgae, both able to supply extra-ATP during steady-state photosynthesis.

Under fluctuating light conditions, growth is severely impaired in *C. reinhardtii flvB* mutants (Fig. 6), as previously observed in *Synechocystis* Δ*flv1* and Δ*flv3* mutants (Allahverdiyeva et al., 2013). This shows that in *C. reinhardtii* the PGR5-PGRL1 CEF is not able to compensate for the loss of Flvs under fluctuating light. In contrast, Arabidopsis growth under fluctuating light relies on the PGRL1/PGR5-mediated CEF, which protects of PSI from photoinhibition in the absence of Flvs (Suorsa et al., 2012), indicating that the overall process of CEF may be more efficient in angiosperms than in algae.

CONCLUSION

While the role of Flv in driving O_2 photoreduction in a photosynthetic organism has been first demonstrated in cyanobacteria (Helman et al., 2003), recent studies performed in the moss *P. patens* (Gerotto et al., 2016) and liverwort (Shimakawa et al., 2017), and mainly based on chlorophyll fluorescence measurements, concluded that Flv drive alternative electron flow and protect PSI particularly under fluctuating light. However, there was no experimental evidence until now of an Flv-catalyzed O_2 photoreduction in microalgae (Curien et al., 2016). Here, by using [^{18}O]-labeled O_2 and MIMS, we clearly establish that Flv are functional in microalgae and involved in O_2 photoreduction. Moreover, quantification of O_2 photoreduction rates showed that Flv massively drives electrons toward O_2 during the induction of photosynthesis. Positive or negative effect of Flv observed on net photosynthesis depending on the fluctuating light conditions, may supply an experimental basis to understand why Flvs were conserved in some species like gymnosperms and algae and discarded in angiosperms. Finally, the loss of Flv in angiosperms could be related to the existence of a more efficient CEF.

MATERIALS AND METHODS

Chlamydomonas Cultures

The *Chlamydomonas reinhardtii* wilt-type strain CC-4533 and *flvB* mutants were obtained from the CLiP (Li et al., 2016). Upon reception, strains were plated on Tris-acetate-phosphate medium and streaked until exhaustion. After a 1-week growth in the dark, three single-clone derived colonies were randomly chosen for conservation and subsequent characterization for each strain. For further liquid culture experiment, cells were grown in flasks at 25°C in HSM medium under dim light (30–40 μmol photon $m^{-2}s^{-1}$). Unless otherwise stated, experiments presented throughout this manuscript were performed on three single colony-derived lines for the wild type and for each of the four strains carrying insertions in the *FLVB* gene; thus, SDs account for SES of biological triplicates calculated with Prism (GraphPad Software).

Spot Tests

Cells were harvested during exponential phase and resuspended in fresh HSM to 2, 10, or 20 μg chlorophyll mL^{-1}. Ten-microliter drops were spotted on plates and exposed to different light regimes. Homogeneous light was supplied by a panel of 400 cool-white LEDs (1 cm distant of each other) and placed 33 cm above plates for growth tests. Temperature was maintained at 25°C at the level of plates by means of fans. The LED panel was powered via a capacitor voltage transformer giving a direct current with a variable voltage between 0 and 54 V. Voltage was monitored via an Arduino UNO microcontroller board to obtain the appropriate light fluctuation regimes.

PCR Procedures

Total DNA was extracted using Chelex kit (Sigma-Aldrich) as described (Dang et al., 2014). Putative insertions were confirmed in three of the four strains by PCR using *TaKaRa LA Taq* DNA polymerase with GC buffer (Clontech). The following set of primers was designed according to Cre16.g691800 gene sequence (Phytozome v5.5; www.phytozome.jgi.doe.gov): F1: 5′-GAGGCATGCGACAGGCCCGAATTGCAC and R2: 5′-GCACGGCACCATCTCCGACCTAGCC for *FLVB* first intron region, F8: 5′-GTACCTGGCTGCAGCGTGTTCACTGCC and R9: 5′-CACCTCGC-AGTAGGTGACCCAGTGGTCG for *FLVB* seventeenth intron region. Cycles were as follows: 2 min at 94°C / 35 cycles: 20 s at 94°C, 20 s at 64°C, 2 min at 72°C/1 min at 72°C. PCR products were separated on 1% (w/v) agarose gels.

Production of FlvB and FlvA Antibodies

Synthetic *FLVA* and *FLVB* genes were cloned respectively into the pLIC7 and the Champion pET151 Directional TOPO (Invitrogen) expression vectors,

allowing the production of a recombinant FLVA fused to TEV-cleavable His-tagged *Escherichia coli* thioredoxin and the recombinant FLVB protein fused to a N-ter $(His)_6$. Production was performed in the *E. coli* BL21 Star (DE3) strain grown at 37°C in TB medium. Induction was initiated at an OD_{600} = 0.6 by adding 0.5 mM isopropyl β-D-thiogalactoside (Sigma-Aldrich). Following overnight incubation at 25°C, cells were centrifuged and pellets resuspended in a lysis buffer containing an antiprotease inhibitor cocktail (SigmaFast tablet), 0.25 mg mL^{-1} lysosyme, and 10 μg mL^{-1} DNaseI. Following incubation (30 min at 4°C), cells were sonicated and centrifuged (12,000*g* for 30 min at 4°C). Crude protein extracts were loaded on a His-Trap HP column (GE Healthcare) and eluted with 250 mM imidazole. The thioredoxin fused to FLVA was cleaved off with overnight incubation with TEV protease. FLVA and FLVB fractions were loaded onto a HiPrep 26/60 Sephadex S-200 HR size-exclusion column (GE Healthcare) and recovered with 10 mM Tris, pH 8.0, buffer containing 300 mM NaCl. The protein peaks containing recombinant FLVA in one case and the $(His)_6$-FlvB in the other case were controlled for purity on SDS-PAGE and concentrated using a Amicon-Ultra device (Millipore). Polyclonal antibodies against FlvA and FlvB were raised in rabbits (ProteoGenix).

Immunodetection

Cells (10–15 mL) were harvested from liquid cultures and centrifuged at 3,000*g* for 2 min. Pellets were then frozen in liquid nitrogen and stored at −20°C until use. Pellets were resuspended in 400 μL 1% SDS and then 1.6 mL acetone (−20°C) was added. After overnight incubation at −20°C, samples were centrifuged (14,000 rpm, 10 min). Supernatant was removed and used for chlorophyll quantification using SAFAS UVmc spectrophotometer (SAFAS). Pellets were resuspended to 1 μg chlorophyll mL^{-1} in LDS in the presence of NuPAGE reducing agent (ThermoFischer) and loaded on 10% PAGE Bis-Tris SDS gel. To load equal protein amounts for immunoblot analysis, protein contents were estimated from Coomassie Brilliant Blue staining using an Odyssey IR Imager (LICOR). After gel electrophoresis, proteins were transferred to nitrocellulose membranes for 90 min at 25 V and 200 mA as described (Dang et al., 2014). Membranes were blocked in milk for 1 h then incubated overnight in the presence of the following antibodies: anti-Cyt *f*, anti-AtpB, anti-PsaD, anti-PsbA, anti-LHCSR3 (Agrisera), or anti-FLVB (see previous paragraph). After 4°C overnight incubation, primary antibody was removed by several rinsings in TBS, and a peroxidase-coupled secondary antibody was added for at least 1 h before detection with a Gbox imaging system (Syngene).

Chlorophyll Fluorescence Measurements

Chlorophyll fluorescence measurements shown in Figures 2, 4, 6, and 7 were performed using a pulse amplitude-modulated fluorimeter (Dual-PAM 100) upon 5-min dark-adaptation under continuous stirring. Detection pulses (10 μmol photon m^{-2} s^{-1} blue light) were supplied at a 100-Hz frequency. Basal fluorescence (F_0) was measured in the dark prior to the first saturating flash. Red saturating flashes (6,000 μmol photon m^{-2} s^{-1}, 600 ms) were delivered to measure F_M (in the dark) and F_M' (in the light). PSII maximum yields were calculated as $(F_M\text{-}F_0)/F_M$. In the experiment shown in Figure 4, DBMIB and MV (Sigma-Aldrich) were added 1 min prior to measurements at final concentrations of 1 μM and 1 mM, respectively. For NPQ measurements (Fig. 7), cells were grown in high light (200 μmol photon m^{-2} s^{-1}) for 24 h to induce LHCSR3 accumulation. Measurements were then performed under 500 μmol photon m^{-2} s^{-1} for 10 min and NPQ calculated as $(F_M-F_M')/F_M'$.

Chlorophyll fluorescence measurements shown in Figure 3 were performed using a Joliot-type spectrofluorimeter (JTS 10; BioLogic). Cells were harvested from flask cultures, centrifuged (3,000 rpm, 2 min), and resuspended in a 3-mL glass cuvette in a buffer containing 20% Ficoll buffered with 20 mM HEPES (pH 7.2). Upon 10 min in the dark, fluorescence was obtained after nonactinic detection pulses of blue light given in the dark (F_0 parameter), during green light saturating flashes (4,000 μmol photon m^{-2} s^{-1}, 250 ms; F_M and F_M' parameters), and during green light illumination at 40, 190, 370, 640, 1,220, and 1,800 μmol photon m^{-2} s^{-1} (F parameter). Maximal PSII yield was calculated from $(F_M-F_0)/F_M$ before illumination, and PSII yield for each light intensity was calculated from $(F_M'-F)/F_M'$.

Absorption Change Measurements

P700 absorption and carotenoid ECS were measured at 705 and 520 nm, respectively, using a JTS-10 (BioLogic). Cells were harvested from flask cultures, centrifuged at 3,000 rpm for 2 min, and resuspended in a 3-mL glass cuvette in a buffer containing 20% Ficoll buffered with 20 mM HEPES (pH 7.2). For P700 absorption change measurements, PSII was inhibited by addition of 3-(3,4-dichlorophenyl)-1,1-dimethylurea (10 μM final concentration), and PSI acceptor side limitations were prevented by addition of oxidized MV, 10 mM final concentration). Measurements were carried out in the dark to reach a baseline level and in response to saturating red light (1,200 μmol photons m^{-2} s^{-1}), $P700^+$ was accumulated within 1 to 2 s. Concentration of oxidizable P700 was calculated from steady-state (~5 s) relative absorbance levels and molar extinction coefficient: $(A_{light}-A_{dark})/(-50*2.3)$ (Hiyama and Ke, 1972; Joliot and Joliot, 2005). P700 absorption changes measured in the absence of MV showed similar results (not shown). For ECS measurements, low light-grown cells were dark-adapted for 5 min in an open cuvette manually bubbled with a syringe (aerobic conditions) and rapidly introduced in the JTS sample holder (BioLogic). ECS was measured during 5 s under orange light (1,170 μmol photons m^{-2} s^{-1}) and normalized to the ECS value measured in response to 6 ns single-turnover flash. Total *pmf* values (ECSt) were calculated from the difference between the ECS value after 5 s in light and the minimum value obtained 300 to 500 ms after light was switched off (Supplemental Fig. S6A). ΔΨ and ΔpH components of the *pmf* were calculated according to the difference between ECSt and maximal ECS value 3 to 5 s after the light was switched off. Using Prism (GraphPad Software), data points of the last seconds of illumination and 0 to 500 ms of dark relaxation were fitted to the "Plateau followed by one-phase decay" function, from which time constants were extracted. Membrane proton conductivity g_H^+ was calculated as the inverse of the time constant and proton flow (ν_H^+) as the product of *pmf* and gH^+ (Cruz et al., 2005).

MIMS Measurements

O_2 exchanges were monitored using a water-jacketed, thermoregulated (25°C) reaction vessel coupled to a mass spectrometer (model Prima dB; Thermo Electron) through a membrane inlet system (Tolleter et al., 2011). The cell suspension (1.5 mL) was placed in the reaction vessel, and bicarbonate (4 mM final concentration) was added to reach CO_2 saturation. [^{18}O]-enriched O_2 (99% $^{18}O_2$ isotope content; Euriso-Top) was bubbled at the top of the suspension until reaching approximately equal concentrations of $^{16}O_2$ and $^{18}O_2$. Upon closure of the reaction vessel, O_2 exchanges were measured during a 2-min dark period, then light was switched on (800 μmol photons m^{-2} s^{-1}). Isotopic O_2 species [$^{18}O^{18}O$] (*m/e* = 36) and [$^{16}O^{16}O$] (*m/e* = 32) were monitored, and O_2 exchange rates were determined as described previously (Radmer and Kok, 1976).

Statistical Analysis

Statistical significance was assessed by ANOVA using GraphPad Prism (GraphPad Software). *P* values were computed by multiple comparison tests using Fischer's LSD test (uncorrected *P* values) or using Tukey corrections for large datasets (adjusted *P* values). Shown are the *P* values or the grouping of strains into statistical families according to *P* values. We defined the statistical significance cutoff as 0.05 (5%).

Supplemental Data

The following supplemental materials are available.

Supplemental Table S1. Wild-type and mutant strains from the CLiP used in this study.

Supplemental Figure S1. PCR characterization of the insertion region in the three *flvB* mutants *flvB-14*, *flvB-208*, and *flvB-308*.

Supplemental Figure S2. Light dependence of PSII yield in wild type and *flvB* mutant strains.

Supplemental Figure S3. Chlorophyll fluorescence kinetics in response to a saturating flash in the wild type and *flvB* mutants.

Supplemental Figure S4. Measurements of dark- and light-induced oxygen uptake rates in the wild type and *flvB* mutant strains.

Supplemental Figure S5. Growth recovery of *flvB* mutants after long exposure to fluctuating light.

Supplemental Figure S6. ECS measurements in the wild-type and *flvB-21* mutant strains.

ACKNOWLEDGMENTS

We thank Claire Riot for preliminary investigations and Drs. Jean Alric and Xenie Johnson (CEA Cadarache) for helpful discussions. Experimental support was provided by the HélioBiotec platform, funded by the European Union (European Regional Development Fund), the Région Provence Alpes Côte d'Azur, the French Ministry of Research, and the CEA.

Received March 29, 2017; accepted May 7, 2017; published May 9, 2017.

LITERATURE CITED

Allahverdiyeva Y, Ermakova M, Eisenhut M, Zhang P, Richaud P, Hagemann M, Cournac L, Aro EM (2011) Interplay between flavodiiron proteins and photorespiration in *Synechocystis* sp. PCC 6803. J Biol Chem **286:** 24007–24014

Allahverdiyeva Y, Isojärvi J, Zhang P, Aro E-M (2015) Cyanobacterial oxygenic photosynthesis is protected by flavodiiron proteins. Life (Basel) **5:** 716–743

Allahverdiyeva Y, Mustila H, Ermakova M, Bersanini L, Richaud P, Ajlani G, Battchikova N, Cournac L, Aro EM (2013) Flavodiiron proteins Flv1 and Flv3 enable cyanobacterial growth and photosynthesis under fluctuating light. Proc Natl Acad Sci USA **110:** 4111–4116

Allen JF (2003) Cyclic, pseudocyclic and noncyclic photophosphorylation: new links in the chain. Trends Plant Sci **8:** 15–19

Badger MR (1985) Photosynthetic oxygen-exchange. Annu Rev Plant Physiol Plant Mol Biol **36:** 27–53

Badger MR, von Caemmerer S, Ruuska S, Nakano H (2000) Electron flow to oxygen in higher plants and algae: rates and control of direct photoreduction (Mehler reaction) and rubisco oxygenase. Philos Trans R Soc Lond B Biol Sci **355:** 1433–1446

Bersanini L, Battchikova N, Jokel M, Rehman A, Vass I, Allahverdiyeva Y, Aro E-M (2014) Flavodiiron protein Flv2/Flv4-related photoprotective mechanism dissipates excitation pressure of PSII in cooperation with phycobilisomes in Cyanobacteria. Plant Physiol **164:** 805–818

Bonente G, Ballottari M, Truong TB, Morosinotto T, Ahn TK, Fleming GR, Niyogi KK, Bassi R (2011) Analysis of LhcSR3, a protein essential for feedback de-excitation in the green alga *Chlamydomonas reinhardtii.* PLoS Biol **9:** e1000577

Chaux F, Johnson X, Auroy P, Beyly-Adriano A, Te I, Cuiné S, Peltier G (2017) PGRL1 and LHCSR3 compensate for each other in controlling photosynthesis and avoiding photosystem I photoinhibition during high light acclimation of *Chlamydomonas* cells. Mol Plant **10:** 216–218

Chaux F, Peltier G, Johnson X (2015) A security network in PSI photoprotection: regulation of photosynthetic control, NPQ and O_2 photoreduction by cyclic electron flow. Front Plant Sci **6:** 875

Cruz JA, Avenson TJ, Kanazawa A, Takizawa K, Edwards GE, Kramer DM (2005) Plasticity in light reactions of photosynthesis for energy production and photoprotection. J Exp Bot **56:** 395–406

Curien G, Flori S, Villanova V, Magneschi L, Giustini C, Forti G, Matringe M, Petroutsos D, Kuntz M, Finazzi G (2016) The water to water cycles in microalgae. Plant Cell Physiol **57:** 1354–1363

DalCorso G, Pesaresi P, Masiero S, Aseeva E, Schünemann D, Finazzi G, Joliot P, Barbato R, Leister D (2008) A complex containing PGRL1 and PGR5 is involved in the switch between linear and cyclic electron flow in *Arabidopsis.* Cell **132:** 273–285

Dang KV, Plet J, Tolleter D, Jokel M, Cuiné S, Carrier P, Auroy P, Richaud P, Johnson X, Alric J, et al (2014) Combined increases in mitochondrial cooperation and oxygen photoreduction compensate for deficiency in cyclic electron flow in *Chlamydomonas reinhardtii.* Plant Cell **26:** 3036–3050

Gerotto C, Alboresi A, Meneghesso A, Jokel M, Suorsa M, Aro E-M, Morosinotto T (2016) Flavodiiron proteins act as safety valve for electrons in *Physcomitrella patens.* Proc Natl Acad Sci USA **113:** 12322–12327

Helman Y, Tchernov D, Reinhold L, Shibata M, Ogawa T, Schwarz R, Ohad I, Kaplan A (2003) Genes encoding A-type flavoproteins are essential for photoreduction of O_2 in cyanobacteria. Curr Biol **13:** 230–235

Hiyama T, Ke B (1972) Difference spectra and extinction coefficients of P 700. Biochim Biophys Acta **267:** 160–171

Johnson X, Steinbeck J, Dent RM, Takahashi H, Richaud P, Ozawa SI, Houille-Vernes L, Petroutsos D, Rappaport F, Grossman AR, et al (2014) PGR5-mediated cyclic electron flow under ATP- or redox-limited conditions: a study of ΔATPase pgr5 and ΔrbcL pgr5 mutants in *Chlamydomonas reinhardtii.* Plant Physiol **165:** 438–452

Joliot P, Johnson GN (2011) Regulation of cyclic and linear electron flow in higher plants. Proc Natl Acad Sci USA **108:** 13317–13322

Joliot P, Joliot A (2005) Quantification of cyclic and linear flows in plants. Proc Natl Acad Sci USA **102:** 4913–4918

Kramer DM, Evans JR (2011) The importance of energy balance in improving photosynthetic productivity. Plant Physiol **155:** 70–78

Li X, Zhang R, Patena W, Gang SS, Blum SR, Ivanova N, Yue R, Robertson JM, Lefebvre PA, Fitz-Gibbon ST, et al (2016) An indexed, mapped mutant library enables reverse genetics studies of biological processes in *Chlamydomonas reinhardtii.* Plant Cell **28:** 367–387

Mehler AH (1951) Studies on reactions of illuminated chloroplasts. I. Mechanism of the reduction of oxygen and other Hill reagents. Arch Biochem Biophys **33:** 65–77

Munekage Y, Hojo M, Meurer J, Endo T, Tasaka M, Shikanai T (2002) PGR5 is involved in cyclic electron flow around photosystem I and is essential for photoprotection in Arabidopsis. Cell **110:** 361–371

Munekage YN, Genty B, Peltier G (2008) Effect of PGR5 impairment on photosynthesis and growth in *Arabidopsis thaliana.* Plant Cell Physiol **49:** 1688–1698

Mustila H, Paananen P, Battchikova N, Santana-Sánchez A, Muth-Pawlak D, Hagemann M, Aro EM, Allahverdiyeva Y (2016) The flavodiiron protein Flv3 functions as a homo-oligomer during stress acclimation and is distinct from the Flv1/Flv3 hetero-oligomer specific to the O_2 photoreduction pathway. Plant Cell Physiol **57:** 1468–1483

Peers G, Truong TB, Ostendorf E, Busch A, Elrad D, Grossman AR, Hippler M, Niyogi KK (2009) An ancient light-harvesting protein is critical for the regulation of algal photosynthesis. Nature **462:** 518–521

Peltier G, Thibault P (1985a) Light-dependent oxygen uptake, glycolate and ammonia release in L-methionine sulfoximide treated *Chlamydomonas.* Plant Physiol **77:** 281–284

Peltier G, Thibault P (1985b) O(2) uptake in the light in chlamydomonas: evidence for persistent mitochondrial respiration. Plant Physiol **79:** 225–230

Peltier G, Tolleter D, Billon E, Cournac L (2010) Auxiliary electron transport pathways in chloroplasts of microalgae. Photosynth Res **106:** 19–31

Radmer RJ, Kok B (1976) Photoreduction of O_2 primes and replaces CO_2 assimilation. Plant Physiol **58:** 336–340

Shikanai T, Yamamoto H (2017) Contribution of cyclic and pseudo-cyclic electron transport to the formation of proton motive force in chloroplasts. Mol Plant **10:** 20–29

Shimakawa G, Ishizaki K, Tsukamoto S, Tanaka M, Sejima T, Miyake C (2017) The liverwort, *Marchantia*, drives alternative electron flow using a flavodiiron protein to protect PSI. Plant Physiol **173:** 1636–1647

Suorsa M, Järvi S, Grieco M, Nurmi M, Pietrzykowska M, Rantala M, Kangasjärvi S, Paakkarinen V, Tikkanen M, Jansson S, et al (2012) PROTON GRADIENT REGULATION5 is essential for proper acclimation of Arabidopsis photosystem I to naturally and artificially fluctuating light conditions. Plant Cell **24:** 2934–2948

Tolleter D, Ghysels B, Alric J, Petroutsos D, Tolstygina I, Krawietz D, Happe T, Auroy P, Adriano JM, Beyly A, et al (2011) Control of hydrogen photoproduction by the proton gradient generated by cyclic electron flow in *Chlamydomonas reinhardtii.* Plant Cell **23:** 2619–2630

Vicente JB, Gomes CM, Wasserfallen A, Teixeira M (2002) Module fusion in an A-type flavoprotein from the cyanobacterium *Synechocystis* condenses a multiple-component pathway in a single polypeptide chain. Biochem Biophys Res Commun **294:** 82–87

Yamamoto H, Takahashi S, Badger MR, Shikanai T (2016) Artificial remodelling of alternative electron flow by flavodiiron proteins in *Arabidopsis*. Nat. Plants **2**: 16012

Zhang P, Allahverdiyeva Y, Eisenhut M, Aro E-M (2009) Flavodiiron proteins in oxygenic photosynthetic organisms: photoprotection of photosystem II by Flv2 and Flv4 in *Synechocystis* sp. PCC 6803. PLoS One **4:** e5331

Zhang P, Eisenhut M, Brandt AM, Carmel D, Silén HM, Vass I, Allahverdiyeva Y, Salminen TA, Aro EM (2012) Operon flv4-flv2 provides cyanobacterial photosystem II with flexibility of electron transfer. Plant Cell **24:** 1952–1971